ESOT | Transplant International

TYPE Original Research
PUBLISHED 11 November 2026
DOI 10.3389/ti.2026.16978

Check for updates

OPEN ACCESS

*CORRESPONDENCE
Aránzazu Caballero-Marcos,
aranzazu.caballero@salud.madrid.org

RECEIVED 20 May 2026
REVISED 07 September 2026
ACCEPTED 06 October 2026
PUBLISHED 11 November 2026

CITATION
Caballero-Marcos A, Díaz-Muñoz L, Puerto M, Alenda R, Ruiz-Martín C, Fernández-Yunquera A, Díaz-Fontenla F, Romero M, Fernández-Martínez M, Morales Á, Duque-González P, Balas A, Bañares R and Salcedo M (2026) PIRCHE-II epitope burden associates with innate immune phenotypes after liver transplantation.
Transpl. Int. 39:16978.
doi: 10.3389/ti.2026.16978

COPYRIGHT
© 2026 Caballero-Marcos, Díaz-Muñoz, Puerto, Alenda, Ruiz-Martín, Fernández-Yunquera, Díaz-Fontenla, Romero, Fernández-Martínez, Morales, Duque-González, Balas, Bañares and Salcedo. This is an open-access article distributed under the terms of the Creative Commons Attribution License (CC BY). The use, distribution or reproduction in other forums is permitted, provided the original author(s) and the copyright owner(s) are credited and that the original publication in this journal is cited, in accordance with accepted academic practice. No use, distribution or reproduction is permitted which does not comply with these terms.

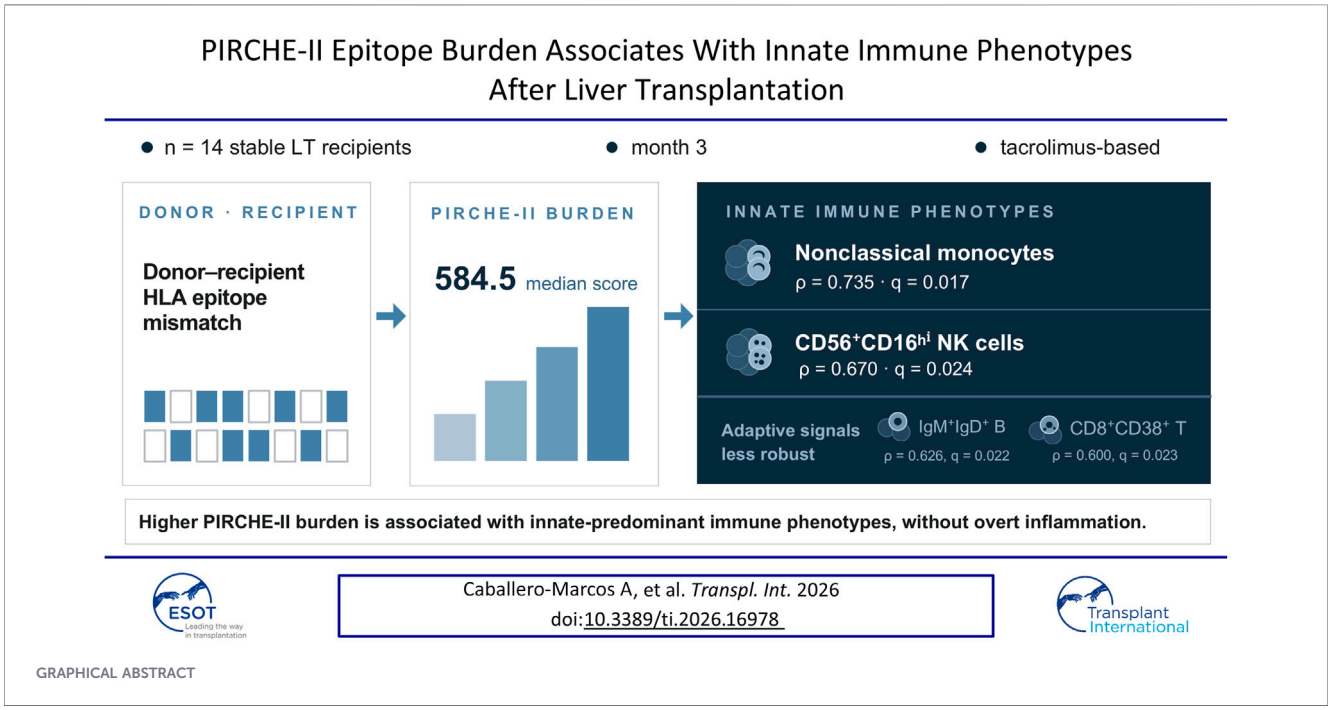
PIRCHE-II epitope burden associates with innate immune phenotypes after liver transplantation

Aránzazu Caballero-Marcos[1]*, Laura Díaz-Muñoz[2], Marta Puerto[3,4], Raquel Alenda[5], Christian Ruiz-Martín[3], Ainhoa Fernández-Yunquera[1], Fernando Díaz-Fontenla[1], Mario Romero[1], María Fernández-Martínez[6], Álvaro Morales[6], Patricia Duque-González[7], Antonio Balas[5], Rafael Bañares[1,4,8] and Magdalena Salcedo[1,4]

[1]Liver Transplant Unit, Department of Gastroenterology and Hepatology, Hospital General Universitario Gregorio Marañón, Madrid, Spain, [2]Flow Cytometry Unit, Instituto de Investigación Sanitaria Gregorio Marañón (IiSGM), Madrid, Spain, [3]Gastroenterology and Hepatology Laboratory, Instituto de Investigación Sanitaria Gregorio Marañón (IiSGM), Madrid, Spain, [4]Centro de Investigación Biomédica en Red de Enfermedades Hepáticas y Digestivas (CIBERehd), Madrid, Spain, [5]Histocompatibility Department, Centro de Transfusión de la Comunidad de Madrid, Madrid, Spain, [6]Department of General and Digestive Surgery, Hospital General Universitario Gregorio Marañón, Madrid, Spain, [7]Department of Anesthesiology and Critical Care, Hospital General Universitario Gregorio Marañón, Madrid, Spain, [8]Faculty of Medicine, Universidad Complutense de Madrid, Madrid, Spain

Whether donor–recipient HLA epitope mismatch burden is associated with specific peripheral immune phenotypes in clinically stable liver transplant (LT) recipients remains unclear. In this exploratory translational study, we evaluated whether HLA epitope mismatch burden, quantified by the PIRCHE-II score, is associated with coordinated peripheral immune configurations in 14 clinically stable LT recipients. Prespecified biologically informed immune cell ratios spanning innate and adaptive compartments were analyzed within a constrained hierarchical framework using Benjamini–Hochberg false discovery rate correction across four primary endpoints; secondary exploratory analyses evaluated broader immune families using within-family correction. Higher PIRCHE-II scores were associated predominantly with innate immune phenotypes, particularly increased proportions of nonclassical monocytes and $CD56^{+}CD16^{high}$ natural killer cells, representing the most robust associations across analytical frameworks, with directionally consistent but statistically attenuated associations observed in $CD8^{+}CD38^{+}$ T cells and $IgM^{+}IgD^{+}$ B-cell compartments in exploratory analyses. These associations occurred without evidence of overt systemic inflammation or major changes in absolute immune cell counts, indicating a qualitative, innate-predominant immune skewing rather than generalized immune activation. These findings support specific and consistent peripheral immune phenotypes associated with epitope mismatch burden in clinically stable LT recipients, although interpretation remains limited by the small sample size and exploratory design.

KEYWORDS
HLA epitope mismatch, immune phenotyping, indirect allorecognition, innate and adaptive immunity, liver transplantation, PIRCHE-II, nonclassical monocytes, natural killer cells



Introduction

Liver transplantation (LT) is characterized by a distinctive immunological profile, with less acute rejection (AR) and greater immune tolerance than other solid organ transplants [1]. Nonetheless, this tolerogenic milieu coexists with persistent low-grade alloimmune heterogeneity, even in clinically stable recipients [2, 3]. This has been linked to progressive graft injury, fibrosis, and late graft dysfunction without overt rejection [4, 5], suggesting that relevant immunological processes may precede clinical events. Accordingly, clinically stable LT may represent a particularly informative setting in which to identify early peripheral immune configurations associated with subclinical alloimmune engagement.

Allorecognition after LT occurs through direct and indirect pathways. While direct allorecognition predominates early after transplantation, the indirect pathway—driven by recipient presentation of donor-derived HLA peptides to $CD4^+$ T cells—has been associated with sustained immune activation, chronic rejection, and antibody-mediated injury [6, 7]. In the liver, continuous antigen exposure within a tolerogenic microenvironment may favor persistent low-grade indirect allorecognition and long-term immune adaptation rather than overt rejection. However, how this epitope-level alloimmune burden is reflected across peripheral innate and adaptive immune phenotypes in clinically stable LT recipients remains incompletely defined. Epitope-based approaches provide a quantitative framework to assess donor–recipient HLA incompatibility beyond conventional antigen-level matching [8].

The Predicted Indirectly Recognizable HLA Epitopes (PIRCHE-II) score estimates the number of donor-derived HLA peptides that can be presented by recipient HLA class II molecules. It provides a quantitative proxy of indirect allorecognition, not a direct measure of immune activation [9]. Higher PIRCHE-II scores have been associated with donor-specific antibodies (DSA) and adverse outcomes in other solid organ transplants [10], although associations with clinical endpoints in adult LT recipients have been inconsistent [11, 12]. Thus, the immunological correlates of PIRCHE-II in LT recipients remain poorly defined.

Although high-dimensional immunophenotyping provides detailed resolution of immune differentiation and activation states, its interpretation is often limited by biological complexity and small sample sizes. In this setting, biologically informed immune ratios provide an analytical framework to integrate related immune features and capture coordinated patterns across immune lineages [13, 14]. Structuring these approaches within biologically related immune families may identify coordinated patterns while limiting analytical redundancy.

Accordingly, rather than evaluating PIRCHE-II as a predictor of clinical outcomes, this study was designed as an exploratory translational analysis to determine whether donor–recipient HLA epitope mismatch burden is associated with peripheral immune phenotypes in clinically stable LT recipients. To our knowledge, this relationship has not previously been examined in LT.

Abbreviations: AR, Acute rejection; BMI, Body mass index; cDC, Conventional dendritic cells; DSA, Donor-specific antibodies; FDR, False discovery rate; HLA, Human leukocyte antigen; ICAM-1, Intercellular adhesion molecule-1; IFN-γ, Interferon gamma; IL, Interleukin; IQR, Interquartile range; LT, Liver transplantation; MASLD, Metabolic-associated steatotic liver disease; MELD, Model for End-Stage Liver Disease; MFI, Mean fluorescence intensity; NK, Natural killer; pDC, Plasmacytoid dendritic cells; PIRCHE-II, Predicted Indirectly Recognizable HLA Epitopes II; PSC, Primary sclerosing cholangitis; PBC, Primary biliary cholangitis; AIH, Autoimmune hepatitis; Treg, Regulatory T cells; TNF-α, Tumor necrosis factor alpha; VCAM-1, Vascular cell adhesion molecule-1.

Patients and methods

Study design and population

This observational exploratory study prospectively enrolled consecutive adult LT recipients at the routine month-3 visit at a single tertiary transplant center. Clinical stability was defined as absence of biopsy-proven acute rejection, clinically significant infection, or graft dysfunction requiring diagnostic or therapeutic intervention; no additional selection criteria were applied. All eligible recipients were included (n = 14); none declined or was unable to participate. Standard early post-transplant immunosuppression adjustments were allowed. Given the exploratory design and small sample, analyses were biologically structured to prioritize signal coherence; no formal sample size calculation was performed.

Peripheral blood samples for immunophenotyping were collected at predefined post-transplant time points as part of a prospective translational research protocol embedded in routine clinical practice. Primary cross-sectional analyses used month-3 samples (~90 days after LT), after most AR episodes occur [15] and beyond the conventional threshold between early and late rejection [16]; restricted to recipients without biopsy-proven rejection, this captures a population beyond the highest early immunological risk while remaining clinically informative. Longitudinal exploratory analyses assessing temporal stability of immune phenotypes between months 3 and 6 were performed in recipients with paired samples available at both time points. Missing data were not imputed, and analyses were performed using available-case data.

The study was conducted in accordance with the Declaration of Helsinki and approved by the local institutional ethics committee. All participants provided written informed consent.

Assessment of HLA epitope mismatch

Donor–recipient HLA epitope mismatch burden was primarily quantified using the PIRCHE-II score, which estimates the number of donor-derived HLA peptides predicted to be processed and presented by recipient HLA class II molecules. The global PIRCHE-II score was defined *a priori* as the primary exposure variable and interpreted as a modeling-based surrogate of indirect alloimmune burden, not a direct functional measure of immune activation. Complete donor and recipient HLA typing data were available for all participants.

As a complementary analysis, the Snow score was calculated as a secondary measure of donor–recipient HLA incompatibility based on B-cell epitope–level surface mismatch, using a previously described computational framework [17]. Because Snow captures class I B-cell epitope mismatch rather than global indirect allorecognition, it was analyzed as a contextual comparator, not a co-primary exposure.

Immunophenotyping and prespecified immune endpoints

Peripheral blood immunophenotyping was performed using multiparameter flow cytometry to characterize innate and adaptive immune cell populations. Immune subsets were primarily expressed as ratios relative to their respective parent populations to capture qualitative immune differentiation while minimizing confounding due to interindividual variability in absolute leukocyte counts. The selection of immune ratios was predefined based on biological plausibility and prior immunological knowledge, rather than data-driven variable selection, in line with recommended analytical approaches for high-dimensional immune profiling [14, 18].

Four immune parameters were defined *a priori* as prespecified primary immune endpoints based on biological plausibility and prior evidence: i) the ratio of nonclassical to total monocytes, reflecting skewing toward a patrolling and vascular-surveillance monocyte phenotype [19]; ii) the ratio of $CD56^{+}CD16^{high}$ to $CD56^{+}CD16^{+}$ natural killer (NK) cells, representing NK-cell functional differentiation [20]; iii) the ratio of $CD8^{+}CD38^{+}$ to total $CD8^{+}$ T cells, as a marker of cytotoxic T-cell activation [21]; and iv) the ratio of $IgM^{+}IgD^{+}$ to total B-cells, capturing compositional remodeling within the naïve-like B-cell compartment [22]. These four endpoints constituted the prespecified primary outcomes; remaining variables were analyzed within predefined exploratory immune families and interpreted descriptively. Detailed immunophenotyping procedures, immune ratio definitions, and analytical grouping strategies are provided in the Supplementary Methods. These ratios were selected *a priori* on biological grounds; one interpretable ratio per lineage (monocyte, NK-cell, T-cell, B-cell) spanned innate and adaptive compartments while limiting primary tests.

Detection of donor-specific antibodies

Serum samples were analyzed for preformed and *de novo* DSA using single-antigen bead assays following standard clinical protocols. Analyses relating DSA status to immune phenotypes were exploratory, descriptive, and intended to generate hypotheses rather than to establish causal relationships.

Statistical analysis

Associations between immune phenotypic variables and HLA epitope mismatch scores were evaluated using Spearman's rank correlation coefficient (ρ), given the small sample size and non-normal distribution of variables. The primary analysis tested associations between the global PIRCHE-II score and the four prespecified immune endpoints, with Benjamini–Hochberg false discovery rate (FDR) correction applied across these four tests [23].

Secondary exploratory analyses evaluated broader immune ratio sets within predefined families, with within-family FDR correction and descriptive interpretation of signal distribution across immune compartments, without redefining primary conclusions. FDR-adjusted q values <0.05 were considered statistically significant, and q values <0.10 were considered suggestive of association.

Additional exploratory analyses related global PIRCHE-II scores and the four prespecified immune ratios to liver

10.3389/ti.2026.16978

TABLE 1 Recipient, donor, and transplant characteristics of the study cohort (n = 14).

Variable	Total (n = 14)
Recipient characteristics	
Age at transplantation, years	62.3 (56.5–64.3)
Male sex	11 (78.6)
MELD-Na score	15 (13–18)
Underlying liver disease	
Alcohol-related liver disease	4 (28.6)
Autoimmune liver disease (PSC/PBC/AIH)	4 (28.6)
MASLD	1 (7.1)
Mixed etiology (alcohol + MASLD)	1 (7.1)
Other	4 (28.6)
Donor characteristics	
Donor age, years	63.0 (39.0–67.0)
Donor BMI, kg/m^2	25.7 (24.4–29.6)
Donor hypertension	3 (21.4)
Donor diabetes mellitus	2 (14.3)
Transplant characteristics	
Donation after brain death	9 (64.3)
Donation after circulatory death	5 (35.7)
Cold ischemia time, min	290 (260–345)
Warm ischemia time, min	30 (28–38)
Static cold storage	9 (64.3)
Normothermic machine perfusion	3 (21.4)
Hypothermic oxygenated perfusion (HOPE)	2 (14.3)
Reperfusion syndrome	3 (21.4)
Immunosuppression	
Induction/initial regimen	
Tacrolimus + corticosteroids (no induction)	7 (50.0)
Basiliximab + MMF + corticosteroids	5 (35.7)
Basiliximab + tacrolimus + corticosteroids	1 (7.1)
Basiliximab + tacrolimus + MMF (steroid-free)	1 (7.1)
Basiliximab induction, any	7 (50.0)
Maintenance at month 3	
Tacrolimus	14 (100)
Tacrolimus trough level, ng/mL	7.75 (5.7–9.5)
Mycophenolate mofetil	6 (42.9)
MMF dose, mg/day	500 (500–1000)
Corticosteroids (prednisone)	12 (85.7)
Prednisone dose, mg/day	5 (5–5)
Everolimus	3 (21.4)
Everolimus trough level, ng/mL	2.6 (2.1–4.8)

Data are presented as median (interquartile range) or number (percentage), as appropriate. MELD-Na score refers to the value at the time of transplantation. Immune phenotyping was performed on peripheral blood samples collected at a standardized post-transplant follow-up time point (month 3 after transplantation). All recipients were clinically stable at the time of sampling, with no evidence of acute rejection, infection, or graft dysfunction requiring intervention. Standard early post-transplant immunosuppression adjustments were permitted. Immunosuppression variables, including trough levels, refer to the month-3, sampling time point.

Abbreviations: MELD-Na, Model for End-Stage Liver Disease including sodium; BMI, body mass index; PSC, primary sclerosing cholangitis; PBC, primary biliary cholangitis; AIH, autoimmune hepatitis; MASLD, metabolic-associated steatotic liver disease; HOPE, hypothermic oxygenated perfusion.

biochemistry and an alloimmune clinical endpoint. Associations with continuous variables were assessed using Spearman's rank correlation coefficient, and comparisons between groups were performed using rank-sum tests. Given the exploratory nature of these analyses and the limited sample size, results were reported descriptively without formal correction for multiple testing.

All analyses were conducted using available-case data without imputation. Statistical analyses were performed using Stata version 16.0 (StataCorp, College Station, TX). Data visualization and figure generation were performed using R software (version 4.5.3; R Foundation for Statistical Computing, Vienna, Austria).

Results

Study population and transplant characteristics

Fourteen adult LT recipients were included. Median age at transplantation was 62.3 years (IQR 56.5–64.3), and the median MELD-Na score was 15 (IQR 13–18). Most grafts were obtained from donors after brain death, and all patients received tacrolimus-based immunosuppression according to institutional protocols. Baseline recipient, donor, and transplant characteristics are summarized in Table 1. No consistent clinical gradients across the range of global PIRCHE-II scores were formally identified.

HLA epitope mismatch burden

The global PIRCHE-II score showed substantial interindividual variability, with a median value of 584.5 (IQR 382.0–689.0). Both HLA class I and class II epitopes contributed to the overall mismatch burden. Among class I loci, contributions from HLA-A, -B, and -C were observed, whereas within class II loci, the highest epitope load was consistently identified at the HLA-DQ locus, followed by DRB and DP. The distribution of global PIRCHE-II scores and class- and locus-specific subscores is detailed in Supplementary Table S1. The median Snow score was 13.0 (IQR 11.0–21.0).

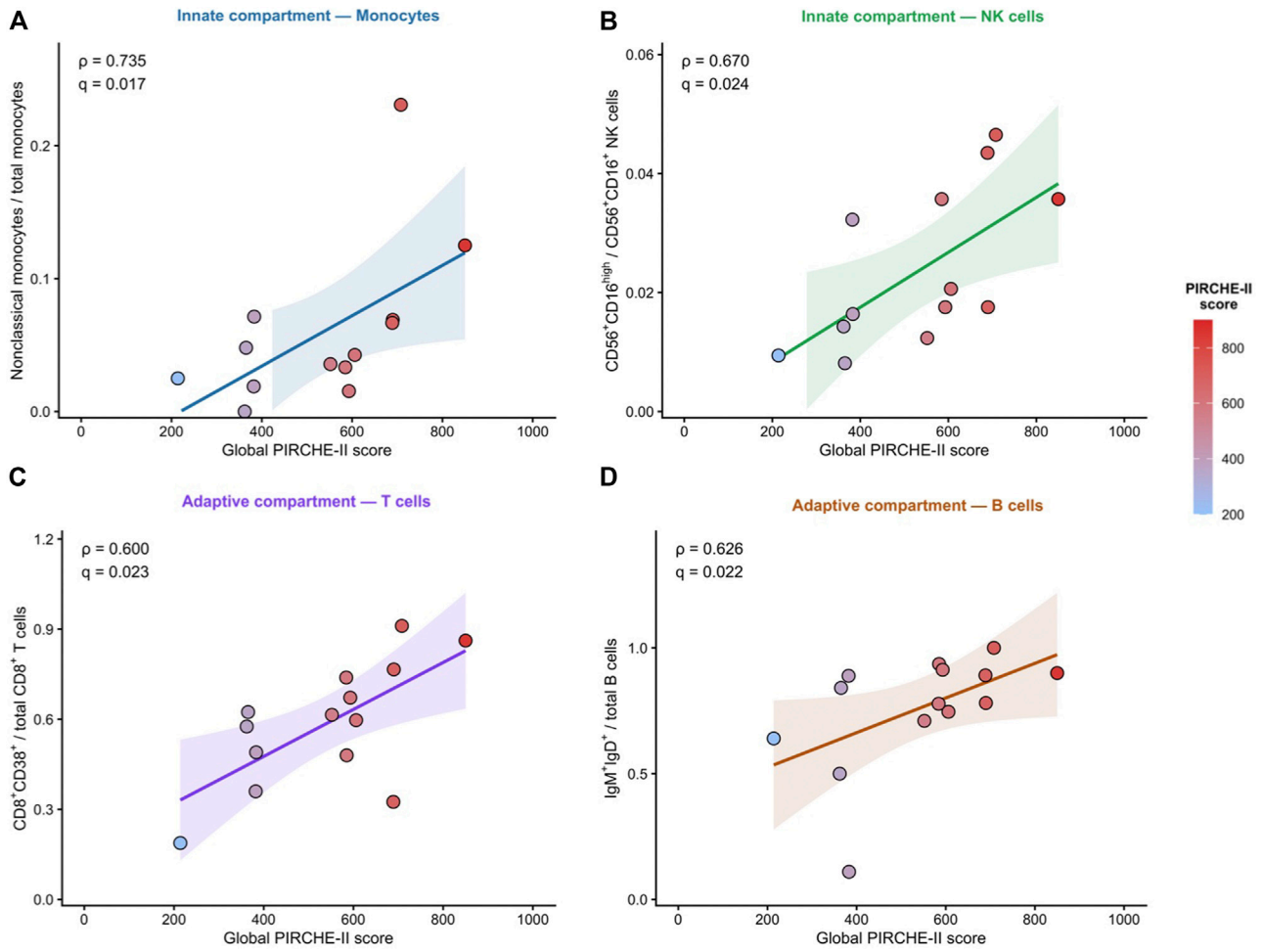


FIGURE 1
Association between global PIRCHE-II epitope mismatch burden and prespecified immune ratio endpoints. Scatter plots depicting the association between the global PIRCHE-II score and four prespecified immune cell ratios. Panel **(A)** shows the ratio of nonclassical monocytes to total monocytes; Panel **(B)**, the ratio of $CD56^{+}CD16^{high}$ to $CD56^{+}CD16^{+}$ natural killer (NK) cells; Panel **(C)**, the ratio of $CD8^{+}CD38^{+}$ activated T cells to total $CD8^{+}$ T cells; and Panel **(D)**, the ratio of $IgM^{+}IgD^{+}$ B cells to total B cells. Each dot represents an individual liver transplant recipient. Dot color reflects global PIRCHE-II burden (blue = lower burden; red = higher burden). Solid lines indicate linear regression fits, and shaded areas represent 95% confidence intervals. Associations were assessed using Spearman's rank correlation; correlation coefficients (ρ) and false discovery rate–adjusted q values (Benjamini–Hochberg correction across the four prespecified endpoints) are shown within each panel. All four prespecified immune ratios showed positive associations with global PIRCHE-II burden. Abbreviations: PIRCHE-II, Predicted Indirectly Recognizable HLA Epitopes; NK, natural killer; FDR, false discovery rate.

Association between HLA epitope mismatch and prespecified immune ratio endpoints

Associations between global PIRCHE-II epitope mismatch burden and the four prespecified immune ratio endpoints are shown in Figure 1. After Benjamini–Hochberg correction across the four prespecified endpoints, higher global PIRCHE-II scores were associated with prespecified immune phenotypes across innate and adaptive compartments within the primary analytical framework.

Specifically, global PIRCHE-II scores were correlated with the proportion of nonclassical monocytes among total monocytes (Spearman ρ = 0.735; FDR-adjusted q = 0.017). A similar association was observed for the ratio of $CD56^{+}CD16^{high}$ to $CD56^{+}CD16^{+}$ NK cells (ρ = 0.670; FDR-adjusted q = 0.024). Within the adaptive immune compartment, higher PIRCHE-II scores showed directionally consistent associations with increased proportions of $IgM^{+}IgD^{+}$ B-cells (ρ = 0.626; FDR-adjusted q = 0.022) and $CD8^{+}CD38^{+}$ phenotypically activated T cells (ρ = 0.600; FDR-adjusted q = 0.023), although these adaptive associations were comparatively less robust and less consistent across exploratory analyses than those observed in innate compartments. All associations were directionally consistent across prespecified endpoints, with the strongest and most robust signals observed in innate immune compartments.

To further contextualize the specificity of these findings, we compared PIRCHE-II with an alternative epitope mismatch framework based on B-cell epitope accessibility (Snow score). As illustrated in Figure 2, PIRCHE-II demonstrated directionally concordant associations across prespecified immune endpoints, whereas the Snow score showed weaker and less consistent associations.

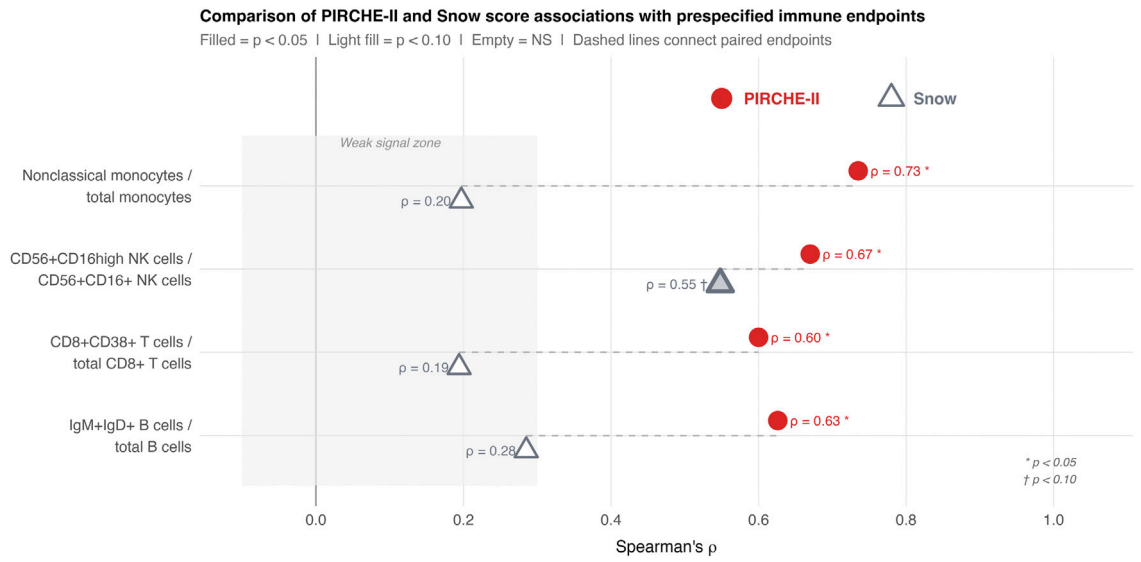


FIGURE 2
Comparative associations of PIRCHE-II and Snow scores with prespecified immune endpoints. Forest plot comparing the associations between two HLA epitope mismatch frameworks—PIRCHE-II and the Snow score—and four prespecified peripheral immune cell ratio endpoints. Each row represents one immune endpoint. Red circles indicate PIRCHE-II associations; grey triangles indicate Snow score associations. Filled symbols denote statistically significant associations ($p < 0.05$); light-filled triangles denote borderline associations ($p < 0.10$); empty symbols denote non-significant associations (NS). Dashed lines connect paired endpoint estimates for each score. Spearman's correlation coefficients (ρ) are shown adjacent to each symbol. Across the four prespecified immune endpoints, PIRCHE-II demonstrated predominantly positive associations, whereas Snow scores showed weaker and less consistent signals, including a borderline association with the $CD56^{+}CD16^{high}$ NK-cell ratio ($\rho = 0.55$; $p = 0.053$). Abbreviations: PIRCHE-II, Predicted Indirectly Recognizable HLA Epitopes; NK, natural killer; NS, non-significant.

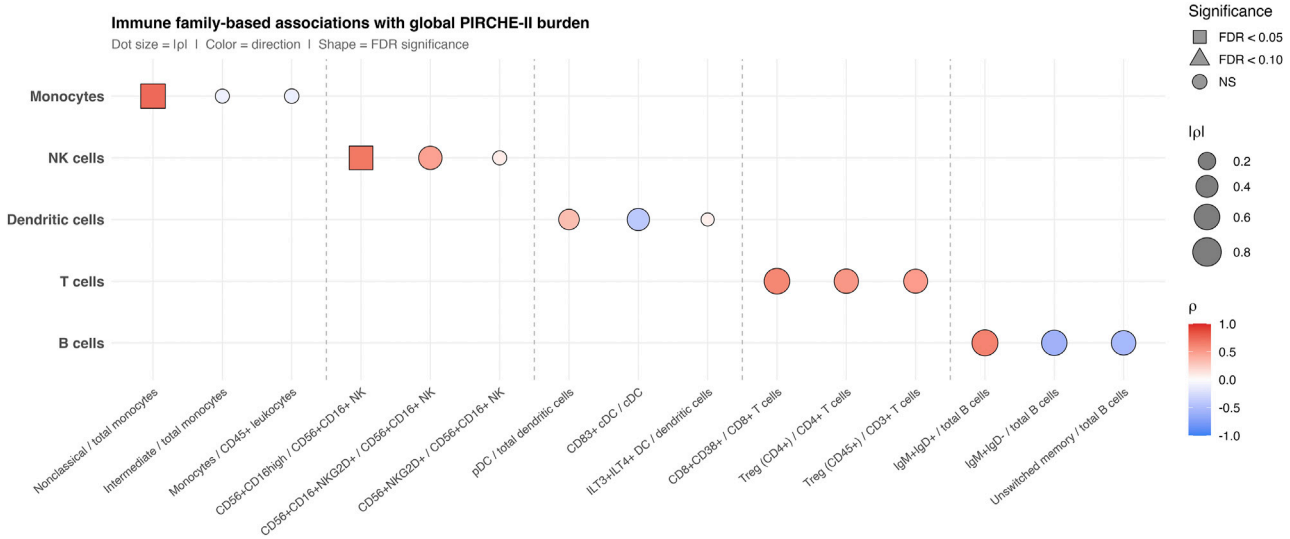


FIGURE 3
Immune family–based overview of associations between global PIRCHE-II epitope mismatch burden and peripheral immune cell ratios. Dot plot summarizing exploratory associations between the global PIRCHE-II score and prespecified immune cell ratios across five immune compartments. Each dot represents one immune ratio endpoint. Dot color indicates the direction and magnitude of Spearman's correlation coefficient (ρ): red denotes positive associations and blue denotes negative associations. Dot size is proportional to the absolute value of ρ. Dot shape indicates false discovery rate (FDR) significance: squares denote FDR $q < 0.05$, triangles denote FDR $q < 0.10$, and circles denote non-significant associations (NS). Dashed vertical lines separate immune family compartments. Associations were predominantly observed within innate immune compartments, particularly monocyte and natural killer (NK)-cell lineages, whereas adaptive immune compartments showed directionally consistent but less robust signals after FDR correction. Analyses are exploratory and hypothesis-generating. Abbreviations: PIRCHE-II, Predicted Indirectly Recognizable HLA Epitopes; NK, natural killer; pDC, plasmacytoid dendritic cells; cDC, conventional dendritic cells; Treg, regulatory T cells; FDR, false discovery rate; ILT, immunoglobulin-like transcript.

Exploratory immune family–based analyses

To assess the internal consistency of the prespecified findings, exploratory analyses were performed within biologically defined immune families using PIRCHE-II as the exposure variable, with FDR correction applied within each lineage. Detailed results are provided in Supplementary Table S2.

Within the monocyte and NK-cell families, the associations between PIRCHE-II and the nonclassical-to-total monocyte ratio and the $CD56^{+}CD16^{high}$ to $CD56^{+}CD16^{+}$ NK-cell ratio, respectively, remained statistically significant after within-family correction. In contrast, no dendritic-cell ratio met the within-family correction threshold. Within the T-cell and B-cell families, several associations were directionally concordant with the prespecified endpoints but did not remain statistically significant after correction for multiple testing.

These exploratory analyses supported the primary findings by showing that the strongest and most consistent associations localized to monocyte and NK-cell compartments, whereas adaptive immune signals were less stable across broader lineage-specific candidate sets.

Figure 3 summarizes the direction and magnitude of associations across immune families. Notably, the strongest and most consistent PIRCHE-II–associated signals were concentrated within innate immune compartments, particularly monocytes and NK cells, whereas adaptive compartments showed weaker and less consistent associations.

Supplementary Tables S1–S3 provide additional exploratory analyses and detailed numerical results.

Exploratory analyses of absolute immune cell counts and detailed subpopulations

Exploratory analyses evaluating associations between global PIRCHE-II scores and absolute immune cell counts did not reveal consistent or systematic correlations across innate or adaptive lineages. Although isolated associations reached nominal significance, they were heterogeneous and not robust after multiple-testing correction. No consistent lineage-wide pattern comparable to immune cell ratios was identified. Detailed results are provided in Supplementary Table S3.

Exploratory analyses of circulating cytokines and endothelial activation markers

Several cytokines classically associated with acute T-cell–mediated immune activation—namely interferon-γ, tumor necrosis factor-α, interleukin-2, and interleukin-17A—were undetectable in the majority of patients and were not included in downstream correlative analyses.

Among the remaining analytes, including IL-4, IL-6, IL-10, ICAM-1, VCAM-1, and E-selectin, associations with immune cell ratios and with global PIRCHE-II scores were heterogeneous and generally modest, without evidence of a consistent lineage-wide pattern and without a systemic inflammatory signature comparable to that observed for immune cell ratios (Supplementary Tables S4, S5).

Association of PIRCHE-II and immune phenotypes with donor-specific antibodies

DSA assessment at month 3 was available in 10 recipients, of whom 2 (20%) exhibited detectable DSA. At month 6, DSA assessment was available in 7 recipients, with DSA detected in 2 (28.6%). Among the six recipients with DSA assessments available at both time points, one patient exhibited persistent DSA from month 3 to month 6, whereas another developed *de novo* DSA at month 6; no cases of DSA disappearance were observed. All DSA detected at month 3 were directed against HLA class II antigens. At month 6, a more heterogeneous humoral profile was observed, with one recipient exhibiting isolated class I DSA and the other displaying combined class I and class II DSA. Among DSA-positive cases, the maximal mean fluorescence intensity of class II DSA was 5325 (IQR 1650–9000) at month 3 and 4800 (IQR 2600–7000) at month 6, whereas class I DSA reached a maximal MFI of 4000.

Recipients with detectable DSA at month 3 showed higher PIRCHE-II scores compared with DSA-negative recipients (median 779 [IQR 708–850] vs. 589 [IQR 467–647.5]). Notably, both DSA-positive recipients exhibited PIRCHE-II values above the interquartile range of DSA-negative patients, suggesting directional separation despite the very small number of DSA-positive cases. Given this limited sample size, this comparison was interpreted as descriptive and hypothesis-generating rather than inferential, despite a nominal p value ($p = 0.037$). The only biopsy-confirmed rejection was a mild acute cellular rejection on day 6 post-transplant, before month-3 sampling and without detectable DSA; one recipient (7.1%) had an early surgical site infection, also before month-3 sampling.

In exploratory analyses, Snow scores showed substantial overlap between DSA-positive and DSA-negative recipients at month 3 (median 17 [IQR 13–21] vs. 13 [IQR 9.5–20.5]; $p = 0.60$).

Exploratory analyses of predefined antigen-presenting cell–related immune ratios according to DSA status at month 3 suggested a consistent directional pattern. Compared with DSA-negative recipients, those with detectable DSA tended to exhibit lower proportions of $ILT3^{+}ILT4^{+}$ dendritic cells relative to total dendritic cells (median 0.24 [IQR 0.09–0.38] vs. 0.40 [IQR 0.19–0.45]) and lower plasmacytoid-to-conventional dendritic cell ratios (median 0.25 [IQR 0.21–0.29] vs. 0.59 [IQR 0.17–0.67]), whereas the proportion of $CD83^{+}$ conventional dendritic cells showed substantial overlap between groups. In addition, DSA-positive recipients displayed higher monocyte-associated CD64-to-CD14 ratios (median 14.28 [IQR 0.78–27.78] vs. 0.23 [IQR 0.06–0.76]). All these comparisons were descriptive and should be interpreted as hypothesis-generating.

Exploratory analyses of clinical and biochemical correlates

To provide additional clinical context for the observed immunophenotypic patterns, exploratory analyses were performed relating global PIRCHE-II burden and the four prespecified immune ratios to graft biochemistry and short-term

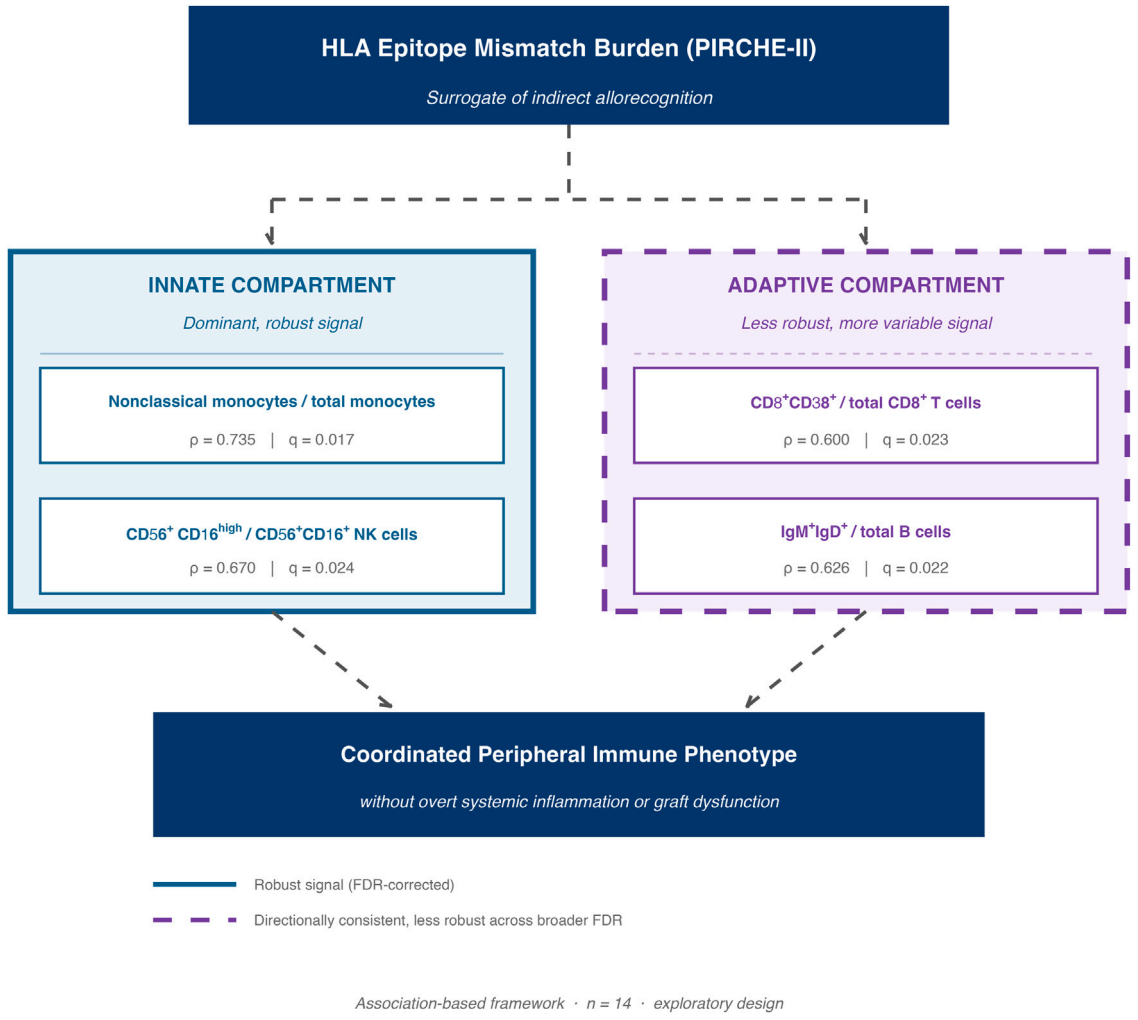


FIGURE 4
Conceptual framework relating HLA epitope mismatch burden to peripheral immune phenotypes in clinically stable liver transplant recipients. Schematic representation of the observed associations between donor–recipient HLA epitope mismatch burden, quantified by the PIRCHE-II score, and peripheral immune phenotypes. Higher PIRCHE-II scores were associated with increased proportions of nonclassical monocytes and $CD56^{+}CD16^{high}$ NK cells (innate immune compartment; predominant and most robust associations) and directionally consistent but less robust associations with $CD8^{+}CD38^{+}$ activated T cells and $IgM^{+}IgD^{+}$ B cells (adaptive immune compartment). These associations occurred in the absence of overt systemic inflammation or graft dysfunction, supporting predominantly qualitative immune phenotypes rather than generalized immune activation. Box border style encodes signal robustness: solid borders indicate associations that remained statistically significant after Benjamini–Hochberg correction across the four prespecified endpoints (FDR $q < 0.05$); dashed borders indicate directionally consistent associations attenuated after correction in broader exploratory analyses. Spearman's correlation coefficients (ρ) and FDR-adjusted q values are shown within each endpoint box. Figure based on observed associations in an exploratory cohort (n = 14); conceptual framework intended for hypothesis generation rather than mechanistic inference. Abbreviations: PIRCHE-II, Predicted Indirectly Recognizable HLA Epitopes; NK, natural killer; FDR, false discovery rate.

longitudinal immune phenotype trajectories between months 3 and 6.

Liver biochemical parameters

Spearman correlations between global PIRCHE-II scores and liver biochemical parameters—alanine aminotransferase, gamma-glutamyltransferase, and bilirubin—at months 3, 6, and 12 were non-significant, with correlation coefficients ranging from −0.19 to 0.28. Correlations between the four prespecified immune ratios and month-3 biochemical parameters were likewise non-significant. The largest observed association was between the $CD56^{+}CD16^{high}$ NK-cell ratio and gamma-glutamyltransferase at month 3 ($\rho = -0.41$; $p = 0.17$).

Longitudinal immune phenotype trajectories

Delta values, calculated as month 6 minus month 3, were assessed for the four prespecified immune ratios in recipients with paired samples available (n = 8 for nonclassical monocytes and NK cells; n = 9 for $CD8^{+}$ T-cells and B-cells). Correlations between global PIRCHE-II scores and longitudinal changes in these immune ratios were uniformly non-significant, without evidence of consistent directional trajectories across immune compartments.

Overall, these exploratory analyses did not identify significant associations beyond the primary immunophenotypic findings, supporting the interpretation that PIRCHE-II–associated immune phenotypes are predominantly subclinical, reflected at the cellular level rather than through overt graft injury.

Discussion

Clinically stable LT recipients represent an immunological setting characterized by relative tolerance and reduced overt rejection responses [5]. In this exploratory study, higher donor–recipient HLA epitope mismatch quantified by the PIRCHE-II score was associated predominantly with innate immune phenotypes despite clinical stability. These associations occurred in the absence of graft dysfunction, systemic inflammation, or major changes in absolute immune cell counts, suggesting predominantly qualitative immune phenotypes rather than generalized immune activation. Importantly, these findings should be interpreted within an exploratory, hypothesis-generating framework rather than as direct clinical inference. The wide interindividual distribution of PIRCHE-II scores highlights heterogeneity in indirect alloimmune potential among LT recipients despite apparent clinical stability [9]. Taken together, our results suggest that epitope-level mismatch is associated with a specific, consistent peripheral immune phenotype that is directionally concordant across innate and adaptive compartments rather than global immune activation. These data do not demonstrate that PIRCHE-II directly determines peripheral immunity; instead, they support an association with specific, internally consistent immune phenotypes under conditions of clinical stability. This interpretation is summarized in Figure 4 as a conceptual, association-based framework rather than a causal mechanistic model.

One of the most robust associations was observed between PIRCHE-II scores and the proportion of nonclassical monocytes. These cells are recognized as mediators of vascular surveillance and immune regulation in settings of sustained immune stimulation [19, 24], and have been described in contexts of low-grade antigenic exposure rather than acute inflammation [25]. Their relative expansion in the present study, in the absence of a systemic inflammatory signature, is consistent with persistent low-level antigenic stimulation rather than overt inflammatory activation. In liver disease, expansion of monocyte and macrophage compartments has been linked to chronic inflammatory signaling and leukocyte recruitment [26], supporting the biological plausibility of this observation after LT. These findings reinforce the predominance of innate immune signals in the observed associations.

Higher PIRCHE-II scores were also associated with a shift toward $CD56^{+}CD16^{high}$ NK cells, a phenotype linked to terminal differentiation and enhanced cytotoxic potential [20, 27]. This occurred without changes in total NK-cell counts, consistent with selective differentiation rather than expansion. Given the liver-enriched biology of NK cells and their roles in rejection and tolerance [28, 29], these findings support epitope mismatch–associated innate immune differentiation.

Within the adaptive immune compartment, PIRCHE-II scores showed directionally consistent associations with increased proportions of $CD8^{+}CD38^{+}$ activated T cells and $IgM^{+}IgD^{+}$ B-cells. However, these associations were less robust than those observed in innate compartments and were attenuated in broader exploratory analyses. CD38 expression on $CD8^{+}$ T-cells reflects recent activation and effector differentiation [21] and has been reported in LT recipients in the absence of rejection [30]. Although CD38 expression alone is not a specific marker of T-cell activation, the association with innate immune ratios and the absence of systemic inflammation argue against nonspecific immune activation. Instead, these findings are more consistent with immune phenotypes involving both innate and adaptive compartments rather than nonspecific immune activation. $IgM^{+}IgD^{+}$ B-cells represent a naïve-like B-cell subset constituting the baseline pool for early humoral responses [22, 31]. Alterations in B-cell composition without overt DSA formation have been described in LT [32, 33], supporting the interpretation of baseline qualitative humoral immune remodeling rather than antibody-mediated injury. Together, these adaptive immune features align with the broader pattern of immune phenotypes observed across innate and adaptive compartments.

Consistent with these cellular findings, cytokines associated with acute T-cell activation, including IFN-γ, TNF-α, IL-2, and IL-17A, were undetectable in most recipients. Clinically stable LT recipients typically exhibit attenuated systemic inflammatory responses despite ongoing antigen exposure [5, 34]. The absence of associations between PIRCHE-II and circulating cytokines or endothelial activation markers suggests that PIRCHE-II–associated immune phenotypes are subclinical and primarily reflected at the cellular level.

Although both PIRCHE-II and Snow represent epitope-level mismatch frameworks, they capture distinct biological dimensions of HLA incompatibility. In this study, only PIRCHE-II showed consistent associations with immune phenotypes. Given these conceptual differences, this comparison should be interpreted as contextual and hypothesis-generating rather than as a formal superiority analysis. PIRCHE-II models donor-derived peptide presentation by recipient HLA class II molecules, approximating indirect allorecognition and $CD4^{+}$ T-cell help [6, 7, 9], mechanisms thought to predominate in late and subclinical alloimmune responses in LT. In contrast, Snow focuses on surface-exposed B-cell epitopes and does not incorporate antigen processing or presentation, which may limit its sensitivity in this setting. These differences may help explain previous reports of inconsistent associations between epitope-based metrics and clinical outcomes in LT [11, 12], suggesting that distinct epitope mismatch frameworks capture different biological layers of alloimmunity.

Exploratory analyses involving DSA were limited by the very small number of DSA-positive cases and were therefore interpreted as descriptive and hypothesis-generating. Early post-transplant DSA were class II–directed and occurred in recipients with higher PIRCHE-II scores, whereas Snow scores showed substantial

overlap according to DSA status. These observations are consistent with, but do not establish, a link between indirect alloimmune burden and early humoral alloimmunity. Importantly, neither liver biochemical parameters nor exploratory clinical correlates demonstrated measurable associations with PIRCHE-II–associated immune phenotypes, supporting the interpretation that these signatures reflect subclinical immune phenotypes rather than clinically overt graft injury in this cohort.

Longitudinal analyses between months 3 and 6 did not identify consistent temporal expansion patterns across immune compartments and should be interpreted cautiously given the limited sample size and exploratory design. These findings suggest that the immunophenotypic differences associated with PIRCHE-II may be more prominently captured at early post-transplant time points rather than through short-term longitudinal dynamics.

Limitations include the modest sample size, single-center design, and lack of hard clinical endpoints, which limit causal inference and preclude robust adjustment for confounders such as immunosuppressive exposure and clinical heterogeneity. The study was designed as an exploratory, hypothesis-generating analysis prioritizing immunological resolution over statistical power, and its findings should be read as biological insight into epitope-associated immune phenotypes rather than evidence of clinical impact. Clinical stability at month 3 does not necessarily reflect immunological quiescence, which was not confirmed by protocol biopsy, so the findings represent cross-sectional associations at a defined early time point. Pre-transplant immunophenotyping was unavailable, limiting our ability to separate pre-existing recipient biology from donor–recipient mismatch; because PIRCHE-II is a property of the specific donor–recipient pairing rather than a recipient-intrinsic trait, however, it is unlikely to track recipient biology alone. Given the absence of a formal sample-size calculation, the significance of all four prespecified endpoints should be interpreted cautiously and requires independent validation. Nevertheless, the use of prespecified endpoints, standardized immunophenotyping, and internal consistency across compartments support the robustness of the observed associations.

In conclusion, donor–recipient HLA epitope-mismatch burden, as captured by PIRCHE-II, is associated with peripheral immune phenotypes in clinically stable LT recipients, with the most robust and reproducible signal localized to innate immune compartments. These associations occur in the absence of systemic inflammation, highlighting the predominantly qualitative nature of epitope mismatch–associated immune differences. Rather than supporting immediate clinical application, these findings provide a conceptual framework relating immunogenetic mismatch to peripheral immune phenotypes post-LT. Further studies integrating immune profiling with longitudinal clinical outcomes are warranted to determine clinical relevance in susceptible LT recipients.

Data availability statement

The raw data supporting the conclusions of this article will be made available by the authors, without undue reservation.

Ethics statement

The studies involving humans were approved by the Clinical Research Ethics Committee (Comité de Ética de la Investigación con Medicamentos, CEIm) of Hospital General Universitario Gregorio Marañón, Madrid, Spain. The studies were conducted in accordance with the local legislation and institutional requirements. The participants provided their written informed consent to participate in this study.

Author contributions

AC-M: Conceptualization, Methodology, Formal analysis, Investigation, Data curation, Writing – original draft, Writing – review and editing, Project administration. LD-M: Investigation, Methodology, Writing – review and editing. MP: Investigation, Methodology, Writing – review and editing. RA: Investigation, Writing – review and editing. CR-M: Investigation, Methodology, Writing – review and editing. AF-Y: Investigation, Writing – review and editing. FD-F: Investigation, Writing – review and editing. MR: Investigation, Writing – review and editing. MF-M: Investigation, Writing – review and editing. AM: Investigation, Writing – review and editing. PD-G: Investigation, Writing – review and editing. AB: Investigation, Writing – review and editing. RB: Supervision, Funding acquisition, Writing – review and editing. MS: Supervision, Funding acquisition, Writing – review and editing. All authors contributed to the article and approved the submitted version.

Funding

The author(s) declared that financial support was received for this work and/or its publication. This work was supported by the Fundación Mutua Madrileña (grant FMM21/02). AC-M is supported by a Juan Rodés contract (JR22/00052) from the Instituto de Salud Carlos III (ISCIII), co-funded by the European Union.

Conflict of interest

The author(s) declared that this work was conducted in the absence of any commercial or financial relationships that could be construed as a potential conflict of interest.

Generative AI statement

The author(s) declared that generative AI was used in the creation of this manuscript. The authors used generative artificial intelligence tools (OpenAI ChatGPT) exclusively for language editing, stylistic refinement, and assistance with manuscript organization. All scientific content, data analysis, interpretation, and final editorial decisions were performed and verified by the authors, who take full responsibility for the accuracy and integrity of the manuscript.

Any alternative text (alt text) provided alongside figures in this article has been generated by Frontiers with the support of artificial intelligence and reasonable efforts have been made to ensure accuracy, including review by the authors wherever possible. If you identify any issues, please contact us.

Supplementary material

The Supplementary Material for this article can be found online at: https://www.frontierspartnerships.org/articles/10.3389/ti.2026.16978/full#supplementary-material

References

1. Thomson AW, Vionnet J, Sanchez-Fueyo A. Understanding, predicting and achieving liver transplant tolerance: from bench to bedside. *Nat Rev Gastroenterol Hepatol* (2020) 17:719–39. doi: 10.1038/s41575-020-0334-4

2. Londoño MC, Souza LN, Lozano JJ, Miquel R, Abraldes JG, Llovet LP, et al. Molecular profiling of subclinical inflammatory lesions in long-term surviving adult liver transplant recipients. *J Hepatol* (2018) 69:626–34. doi: 10.1016/j.jhep.2018.04.012

3. Vionnet J, Miquel R, Abraldes JG, Wall J, Kodela E, Lozano JJ, et al. Non-invasive alloimmune risk stratification of long-term liver transplant recipients. *J Hepatol* (2021) 75:1409–19. doi: 10.1016/j.jhep.2021.08.007

4. Sánchez-Fueyo A, Strom TB. Immunological tolerance and liver transplantation. *J Hepatol* (2004) 41:698–705. doi: 10.1016/j.jhep.2004.09.013

5. Sánchez-Fueyo A, Strom TB. Immunologic basis of graft rejection and tolerance following transplantation of liver or other solid organs. *Gastroenterology* (2011) 140: 51–64. doi: 10.1053/j.gastro.2010.10.059

6. Game DS, Lechler RI. Pathways of allorecognition: implications for transplantation tolerance. *Transpl Immunol* (2002) 10:101–8. doi: 10.1016/s0966-3274(02)00055-2

7. Afzali B, Lombardi G, Lechler RI. Pathways of major histocompatibility complex allorecognition. *Curr Opin Organ Transpl* (2008) 13:438–44. doi: 10.1097/MOT.0b013e328309ee31

8. Tambur AR, Claas FHJ. HLA epitopes as viewed by antibodies: what is it all about? *Am J Transpl* (2015) 15:1148–54. doi: 10.1111/ajt.13192

9. Geneugelijk K, Spierings E. PIRCHE-II: an algorithm to predict indirectly recognizable HLA epitopes in solid organ transplantation. *Immunogenetics* (2020) 72:119–29. doi: 10.1007/s00251-019-01140-x

10. Lachmann N, Niemann M, Reinke P, Budde K, Schmidt D, Halleck F, et al. Donor-recipient matching based on predicted indirectly recognizable HLA epitopes independently predicts the incidence of *de novo* donor-specific HLA antibodies following renal transplantation. *Am J Transpl* (2017) 17:3076–86. doi: 10.1111/ajt.14393

11. Kok G, Verstegen MMA, Houwen RHJ, Nieuwenhuis EES, Metselaar HJ, Polak WG, et al. Assessment of human leukocyte antigen matching algorithm PIRCHE-II on liver transplantation outcomes. *Liver Transpl* (2022) 28:1356–66. doi: 10.1002/lt.26431

12. Kubal CA, Mangus R, Ekser B, Mihaylov P, Ceballos B, Higgins N, et al. Class II human leukocyte antigen epitope mismatch predicts *de novo* donor-specific antibody formation after liver transplantation. *Liver Transpl* (2018) 24:1101–8. doi: 10.1002/lt.25286

13. Maecker HT, McCoy JP, Nussenblatt R. Standardizing immunophenotyping for the human immunology project. *Nat Rev Immunol* (2012) 12:191–200. doi: 10.1038/nri3158

14. Aghaeepour N, Finak G, Hoos H, Mosmann TR, Brinkman R, Gottardo R, et al. Critical assessment of automated flow cytometry data analysis techniques. *Nat Methods* (2013) 10:228–38. doi: 10.1038/nmeth.2365

15. Wiesner RH, Demetris AJ, Belle SH, Seaberg EC, Lake JR, Zetterman RK, et al. Acute hepatic allograft rejection: incidence, risk factors, and impact on outcome. *Hepatology* (1998) 28:638–45. doi: 10.1002/hep.510280306

16. Thurairajah PH, Carbone M, Bridgestock H, Thomas P, Hebbar S, Gunson BK, et al. Late acute liver allograft rejection: a study of its natural history and graft survival in the current era. *Transplantation* (2013) 95:955–9. doi: 10.1097/TP.0b013e3182845f6c

17. Niemann M, Matern BM, Spierings E. Snowflake: a deep learning-based human leukocyte antigen matching algorithm considering allele-specific surface accessibility. *Front Immunol* (2022) 13:937587. doi: 10.3389/fimmu.2022.937587

18. Spitzer MH, Nolan GP. Mass cytometry: single cells, many features. *Cell* (2016) 165: 780–91. doi: 10.1016/j.cell.2016.04.019

19. Cros J, Cagnard N, Woollard K, Patey N, Zhang SY, Senechal B, et al. Human CD14dim monocytes patrol and sense nucleic acids and viruses *via* TLR7 and TLR8 receptors. *Immunity* (2010) 33:375–86. doi: 10.1016/j.immuni.2010.08.012

20. Lopez-Vergès S, Milush JM, Pandey S, York VA, Arakawa-Hoyt J, Pircher H, et al. CD57 defines a functionally distinct population of mature NK cells in the human CD56dimCD16+ NK-cell subset. *Blood* (2010) 116:3865–74. doi: 10.1182/blood-2010-04-282301

21. Sandoval-Montes C, Santos-Argumedo L. CD38 is expressed selectively during the activation of a subset of mature T cells with reduced proliferation but improved potential to produce cytokines. *J Leukoc Biol* (2005) 77:513–21. doi: 10.1189/jlb.0404262

22. Sims GP, Ettinger R, Shirota Y, Yarboro CH, Illei GG, Lipsky PE. Identification and characterization of circulating human transitional B cells. *Blood* (2005) 105:4390–8. doi: 10.1182/blood-2004-11-4284

23. Benjamini Y, Hochberg Y. Controlling the false discovery rate: a practical and powerful approach to multiple testing. *J R Stat Soc Ser B Stat Methodol* (1995) 57: 289–300. doi: 10.1111/j.2517-6161.1995.tb02031.x

24. Ziegler-Heitbrock L. The CD14+ CD16+ blood monocytes: their role in infection and inflammation. *J Leukoc Biol* (2007) 81:584–92. doi: 10.1189/jlb.0806510

25. Wong KL, Yeap WH, Tai JJY, Ong SM, Dang TM, Wong SC. The three human monocyte subsets: implications for health and disease. *Immunol Res* (2012) 53:41–57. doi: 10.1007/s12026-012-8297-3

26. Zimmermann HW, Seidler S, Gassler N, Nattermann J, Luedde T, Trautwein C, et al. Interleukin-8 is activated in patients with chronic liver diseases and associated with hepatic macrophage accumulation in human liver fibrosis. *PLoS One* (2011) 6:e21381. doi: 10.1371/journal.pone.0021381

27. Björkström NK, Riese P, Heuts F, Andersson S, Fauriat C, Ivarsson MA, et al. Expression patterns of NKG2A, KIR, and CD57 define a process of CD56dim NK-cell differentiation uncoupled from NK-cell education. *Blood* (2010) 116:3853–64. doi: 10.1182/blood-2010-04-281675

28. Harmon C, Sanchez-Fueyo A, O'Farrelly C, Houlihan DD. Natural killer cells and liver transplantation: orchestrators of rejection or tolerance? *Am J Transpl* (2016) 16: 751–7. doi: 10.1111/ajt.13565

29. Male V, Stegmann KA, Easom NJ, Maini MK. Natural killer cells in liver disease. *Semin Liver Dis* (2017) 37:198–209. doi: 10.1055/s-0037-1603946

30. Demetris AJ, Adeyi O, Bellamy COC, Clouston A, Charlotte F. Liver biopsy interpretation for causes of late liver allograft dysfunction. *Hepatology* (2006) 44: 489–501. doi: 10.1002/hep.21280

31. Wirths S, Lanzavecchia A. ABCB1 transporter discriminates human resting naive B cells from cycling transitional and memory B cells. *Eur J Immunol* (2005) 35:3433–41. doi: 10.1002/eji.200535364

32. Martínez-Llordella M, Lozano JJ, Puig-Pey I, Orlando G, Tisone G, Lerut J, et al. Using transcriptional profiling to develop a diagnostic test of operational tolerance in liver transplant recipients. *J Clin Invest* (2008) 118:2845–57. doi: 10.1172/JCI35342

33. Caballero-Marcos A, Salcedo M, Alonso-Fernández R, Rodríguez-Perálvarez M, Olmedo M, Graus Morales J, et al. Changes in humoral immune response after SARS-CoV-2 infection in liver transplant recipients compared to immunocompetent patients. *Am J Transpl* (2021) 21:2876–84. doi: 10.1111/ajt.16599

34. Gao B, Jeong WI, Tian Z. Liver: an organ with predominant innate immunity. *Hepatology* (2008) 47:729–36. doi: 10.1002/hep.22034